Layer-by-Layer Assembly of Thin Film Zener Diodes from Conducting Polymers and CdSe Nanoparticles

Thierry Cassagneau,[†] Thomas E. Mallouk,[†] and Janos H. Fendler*,[‡]

Contribution from the Department of Chemistry, 152 Davey Laboratory, The Pennsylvania State University, University Park, Pennsylvania 16802, and Center for Advanced Materials Processing, Clarkson University, P.O. Box 5814, Potsdam, New York 13699-5814

Received February 23, 1998

Abstract: Ultrathin films have been prepared by self-assembling trioctylphosphine oxide, TOPO, capped n-type 20−40 Å diameter CdSe nanoparticles and 1,6-hexadecanethiol, HDT, onto p-doped semiconducting polymers, chemically deposited poly(3-methylthiophene), PMeT (for ***Device A***), and electrochemically deposited poly-(pyrrole), Ppy (for ***Device B***). The semiconducting polymers have, in turn, been electrochemically layered (for ***Device A***) or layer-by-layer chemically assembled (for ***Device B***) onto derivatized conducting substrates. The ultrathin films have been characterized by absorption and emission spectroscopy, transmission electron microscopy, scanning force microscopy, X-ray photoelectron spectroscopy, and by electrochemical measurements. By controlling the level of doping into the p-type junction, it was possible to prepare dissymmetrical junctions and observe a rectifying behavior in the forward direction and a Zener breakdown in the reverse direction for Au/PMeT/(HDT/CdSe)$_3$, ***Device A***, and for Au/MEA/Ppy/(HDT/CdSe)$_3$, ***Device B***. Additionally, Au/MeA/PAH/CdSe (PAH = poly(allylamine hydrochloride)), Au/MEA/Ppy/PSS/CdSe (PSS = polystyrene sulfonate), and Au/MEA/Ppy/α-ZrP/CdSe (α-ZrP = α zirconium phosphate) films have been prepared and characterized.

Introduction

Size quantization of semiconductor nanoparticles manifest itself in markedly altered physical and chemical behavior.[1−6] In particular, size dependent changes in mechanical, optical, electrical, electrooptical, magnetic, and magnetooptical properties have been observed.[7,8] Exploitation of the beneficial properties of nanoparticles for device construction requires that they are organized into high density two-dimensional arrays and/or three-dimensional networks in which suitable electrical contact can be made and in which the current, voltage, and/or light intensity can be measured. The layer-by-layer self-assembly (adsorption)[9] of oppositely charged polyelectrolytes,[10] polyelectrolytes and nanoparticles,[11,12a] polyelectrolytes and graphite oxide,[12b] polyelectrolytes and layered α-zirconium phosphate nanoplatelets,[13] and polyelectrolytes and clay platelets[12,14] have provided an eminently suitable approach to the construction of ultrathin films. That any number of layers of nanoparticles (or platelets) of any composition can be adsorbed in any desired order ensures the versatility of ultrathin film construction by the self-assembly method.

The availability of appropriate semiconductor nanoparticles and polyelectrolytes has opened the door to the construction of a new class of electroluminescent devices[7,15−18] including a multicolor pixel voltage-controllable light-emitting diode.[7] In this approach, a rectifying p−n junction has been fabricated from a p-type semiconducting polymer, SCP (poly(*p*-phenylene

[†] The Pennsylvania State University.
[‡] Clarkson University.

(1) Fendler, J. H., *Membrane Mimetic Approach to Advanced Materials*; Springer-Verlag: Berlin, 1992.
(2) Fendler, J. H.; Meldrum, F. C. *Adv. Mater*. **1995**, *7*, 607.
(3) Alivisatos, A. P. *Materials Research Society Bulletin* **1995**, *XX*, 23.
(4) Henglein, A. *Ber. Bunseng. Phys. Chem*. **1995**, *99*, 903.
(5) Hodes, G. *Solar Energy Materials and Solar Cells* **1994**, *32*, 323.
(6) Weller, H. *Angew. Chem., Int. Ed. Engl*. **1993**, *32*, 41.
(7) Colvin, V. L.; Schlamp, M. C.; Alivisatos, A. P. *Nature* **1994**, *370*, 354.
(8) Cheung, J. H.; Fou, A. F.; Rubner, M. F. *Thin Solid Films* **1994**, *244*, 985.
(9) Decher, G. In *Comprehensive Supramolecular Chemistry*; Sauvage, J.-P., Ed.; Pergamon Press: Oxford, 1996; pp 507−528.
(10) (a) Decher, G.; Hong, J.-D. *Makromol. Chem*. **1991**, *46*, 321. (b) Decher, G.; Hong, J.-D.; Schmitt, J. *Thin Solid Films* **1992**, *210/211*, 504. (c) Decher, G.; Schmitt, J. *Prog. Colloid Polym. Sci*. **1992**, *89*, 160. (d) Lvov, Y.; Decher, G.; Môhwald, H. *Langmuir* **1993**, *9*, 481. (e) Lvov, Y.; Decher, G.; Sukhorukov, G. *Macromolecules* **1993**, *26*, 5396. (f) Lvov, Y.; Essler, F.; Decher, G. *J. Phys. Chem*. **1993**, *97*, 13773. (g) Schmitt, J.; Grünewald, T.; Kjaer, K.; Pershan, P.; Decher, G.; Lösche, M. *Macromolecules* **1993**, *26*, 7058.
(11) (a) Schmitt, J.; Decher, G.; Dressick, W. J.; Brandow, S. L.; Geer, R. E.; Shashidhar, R.; Calvert, J. M. *Adv. Mater*. **1997**, *9*, 61. (b) Ariga, K.; Lvov, Y.; Onda, M.; Ichinose, I.; Kunitake, T. *Chem. Lett*. **1997**, 125. (c) Liu, Y.; Wang, A.; Claus, R. O. *Appl. Phys. Lett.* **1997**, *71*, 2265.
(12) (a) Kotov, N. A.; Dékány, I.; Fendler, J. H. *J. Phys. Chem*. **1995**, *99*, 13065. (b) Kotov, N. A.; Dékány, I.; Fendler, J. H. *Adv. Mater*. **1996**, *8*, 637. (c) Kotov, N. A.; Haraszti, T.; Turi, L.; Zavala, G.; Geer, R. E.; Dékány, I.; Fendler, J. H. *J. Am. Chem. Soc*. **1997**, *119*, 6821.
(13) (a) Keller, S. W.; Kim, H.-Y.; Mallouk, T. E. *J. Am. Chem. Soc*. **1994**, *116*, 8816. (b) Keller, S. W.; Johnson, S. A.; Brigham, E. S.; Yonemoto, E. H.; Mallouk, T. E. *J. Am. Chem. Soc*. **1995**, *117*, 12879. (c) Kim, H.-N.; Keller, S. W.; Mallouk, T. E.; Smitt, J.; Decher, G. *Chem. Mater*. **1997**, *9*, 1414.
(14) (a) Kleinfeld, E. R.; Ferguson, G. S. *Science* **1994**, *265*, 370. (b) Kleinfeld, E. R.; Ferguson, G. S. *Adv. Mater*. **1995**, *7*, 414. (c) Kleinfeld, E. R.; Ferguson, G. S. *Mater. Res. Soc. Symp*. **1995**, *369*, 697. (d) Kleinfeld, E. S.; Ferguson, G. S. *Chem. Mater*. **1996**, *8*, 1575.
(15) (a) Dabbousi, B. O.; Murray, C. B.; Rubner, M. F.; Bawendi, M. G. *Chem. Mater*. **1994**, *6*, 216. (b) Dabbousi, B. O.; Bawendi, M. G.; Onitsuka, O.; Rubner, M. F. *Appl. Phys. Lett*. **1995**, *66*, 1316.
(16) (a) Colvin, V. L.; Alivisatos, A. P. *Phys. Rev. Lett*. **1991**, *66*, 2786. (b) Colvin, V. L.; Goldstein, A. N.; Alivisatos, A. P. *J. Am. Chem. Soc*. **1992**, *114*, 5221.
(17) Gao, M.; Richter, B.; Kirstein, S. *Adv. Mater*. **1997**, *9*, 802.
(18) Kumar, N. D.; Joshi, M. P.; Friend, C. S.; Prasad, P. N.; Burzynski, R. *Appl. Phys. Lett*. **1997**, *71*, 1388.

S0002-7863(98)00602-7 CCC: $15.00
Published on Web 07/28/1998

vinylene), PPV, for example), layer and an n-type semiconductor (cadmium selenide, CdSe, for example) nanoparticle layer. These ultrathin films serving as p−n junctions have been constructed by self-assembly (alternating layers of CdSe nanoparticles stabilized by 1,6-hexanedithiol and PPV),[7] by the Langmuir−Blodgett technique (transferring the CdSe nanoparticles to glass slides coated with a layer of sulfonated polystyrene),[15a] and by spin-casting (after mixing the nanoclusters with poly(vinylcarbazole) as a hole conducting polymer and an oxadiazole derivative, t-Bu-PBD as the electron transport agent).[15b]

In addition to the rectifying behavior expected for such a Schottky-type junction, one can also design, in principle, a Zener junction by creating an asymmetry in the degree of doping of the electroactive layers. For example, one can envisage to control, chemically or electrochemically, the degree of p-doping in the SCP without affecting the properties of the n-type semiconductor nanoparticle layer. Such a Zener junction cannot be constructed exclusively from semiconducting polymers because p- and n-types of doping cannot be separately introduced to neighboring layers. Additionally, n-doped SCP (polypyrrole or polythiophene, for example) tend to become dedoped upon exposure to air.[19] This problem can be overcome by coupling the p-type SCP to an n-type semiconductor nanoparticle layer.

Encouraged by the reported successful construction of nanoparticle based electroluminescence devices[7,15,16] we have undertaken a systematic investigation of the assembling and self-assembling advanced electronic devices. Here, we report the results of our study on two p−n junction based devices (***Device A*** and ***Device B***) which are both rectifying and can undergo a Zener breakdown. The p-type layer was constructed from SCPs, using poly(3-methylthiophene) for ***Device A*** and poly(pyrrole) for ***Device B***. Self-assembled arrays of CdSe nanoparticles constituted the n-type layer for both ***Device A*** and ***Device B***. Very similar behavior was observed for the two devices upon the doping of the SCP. Applying a positive forward bias caused rectification which followed the Fowler−Nordheim law, characteristic of charge injection by tunneling mechanism. Upon applying a negative bias a Zener breakdown occurred which was attributed to dissymmetrical doping of the n-type (the self-assembled arrays of CdSe nanoparticles) and the p-type (the SCP) layers assembled in the ultrathin film.

Experimental Section

Materials. Dimethylcadmium (99+%, Strem), 1,6-hexanedithiol (>97%, Fluka, HDT), HCl (36.5−38%, Baker), and (4-aminobutyl)-dimethylmethoxysilane (United Chemical Technologies, Inc., AMS) were used as received. Poly(styrene-4-sulfonic acid), sodium salt, PSS, 20% solution in water, was obtained from Aldrich; before use it was diluted to 0.02 M concentration with 0.01 M HCl. Pyrrole (98%), selenium powder (100 mesh, 99.999%), trioctylphosphine (90%, TOP), trioctylphosphine oxide (99%, TOPO), tetrabutylammonium tetrafluoroborate (99%), 2-aminoethanethiol hydrochloride (98%), 3-methylthiophene (98%), $FeCl_3 \cdot 6H_2O$ (98%), anhydrous ethyl alcohol, anhydrous butanol (99.5%), anhydrous benzonitrile (99+%), anhydrous powder of lithium tetrafluoroborate (99.999%), Rhodamine B, poly(allylamine hydrochloride) (M_w = 50 000−65 000), and mercaptoethylamine hydrochloride (98%, MEA) were purchased from Aldrich and used without further purification. Distilled water was put through a Barnstead Nanopure II column to obtain deionized water with a resistivity of 18 MW·cm. Quartz slides was obtained from Chemglass, Inc., and conducting Indium Tin Oxide, ITO, coated glass was purchased from Delta Technologies, White Bear Lake, MN. Gold substrates were purchased from EMF Corp. (Ithaca, NY) and consisted of a 1000 Å gold layer deposited onto a glass covered with a thin layer of titanium (50 Å). These substrates were exposed to a fresh piranha solution (75% H_2SO_4/25% H_2O_2) for 5−10 min and were copiously washed with deionized water prior to using them. α Zirconium phosphate, α-$Zr(H_2PO_4)_2 \cdot H_2O$ (α-ZrP) has been prepared by the direct precipitation method.[20a] The colloidal suspension used in self-assembly resulted from the exfoliation of α-ZrP in an aqueous solution of propylamine as previously reported.[20b]

Instrumentation. Absorption spectra were recorded on a Hewlett-Packard 8452A diode array spectrophotometer. Ellipsometric data were acquired by using a Gaertner Model L2W26D ellipsometer with a HeNe laser (632.8 nm) light source. For measurements, the real part of the refractive index was fixed to 1.54, while the imaginary part was assumed to be zero. Thicknesses data were averaged values obtained from different spots (5−6) on a given sample. Transmission electron microscopy images were obtained by using a JEOL 1200 EXII microscope operating at 120 kV. X-ray photoelectron spectra (XPS) were determined by a Hewlett-Packard 5950A instrument with 256 multichannel resistor plates. Spectra were taken using the Al K_a line source at 1486.6 eV. Approximate compositions were obtained from simple curve fits of the Se 3s/s 2s envelope. Interference between the S 2p peak (the most intense photoelectron peak for S) and other peaks (Se 3p and Al X-ray ghosts from the Cd 3d peak, which were comparable in size and very close to it) prevented the use of the conventional fitting. Unfortunately, the uncertainty in the S concentration was as high as ±20%, making an evaluation difficult. Additional carbon was present due to storing samples in air for 20 months. Therefore, the XPS results reported here should be considered qualitative. Atomic force microscopic (AFM) was performed with a Digital Nanoscope IIIa system. The pyramidal AFM tips and cantilevers were made from etched silicon probes. All AFM images were collected in tapping mode in air, resonating the tip just below the oscillation frequency of the cantilever (typically 250−325 kHz). The scanning frequency was 1−2 Hz, and the data collection resolution was 512 × 512 pixels. Tips were changed frequently to maintain the resolution of the AFM images. Electrochemical syntheses were performed under Ar atmosphere by using a Princeton Applied Research Model 273 potentiostat. The working electrode consisted of a gold (or ITO) substrate while auxiliary and reference electrodes were platinum and Ag/Ag^+ respectively. $i-V$ characteristics were obtained in air, at room temperature, after evaporation of an Al film (several hundreds of Å) on multilayers deposited onto gold substrates, by using a potentiostat (same model) interfaced with a MacLab electrochemical software version 1.3. Fluorescence spectra were obtained with a Spex Fluorolog 1681 fluorometer at room temperature using front face observations.

Methods

Substrate Derivatization. Both ITO and gold substrates were pretreated by an appropriate molecule which could act as anchoring agent for the semiconducting polymer by virtue of their pH sensitive terminal amino groups. ITO substrates were pretreated by (i) overnight (ca. 15 h) immersion into a 0.3 M solution of (4-aminobutyl)dimethylmethoxysilane in toluene (in a desiccator) and (ii) washing with toluene, ethanol, and water to provide an 8 ± 1 Å thick (determined by ellipsometry) coating. Gold substrates were pretreated by (i) immersion into a 2% (w/v) aqueous 2-mercaptoethylamine hydrochloride solution for 12−15 h, (ii) washing by and sonicating in ethanol, and (iii) washing with water to provide an 8 ± 1 Å thick (determined by ellipsometry) coating.

Preparation of Polypyrrole, Ppy. Pyrrole monomer can be oxidized at ca. +0.6−0.8 V vs SCE, thereby initiating the formation of poly(pyrrole). The polymer is made in the oxidized

(19) (a) de Leeuw, D. M.; Simenon, M. M. J.; Brown, A. R.; Einerhand, R. E. F. *Synthetic Metals* **1997**, *87*, 53. (b) Chowdhury, A.-N.; Harima, Y.; Kunugi, Y.; Yamashita, K. *Electrochim. Acta* **1996**, *41*, 1993.

(20) (a) Alberti, G.; Torracca, E. *J. Inorg. Nucl. Chem.* **1968**, *30*, 317. (b) Alberti, G.; Casciola, M.; Costantino, U. *J. Colloid Interface Sci.* **1985**, *107*, 256.

form and can be reduced at potentials negative of 0.0 V vs SCE. It is reoxidized at potentials positive of about +0.2 V vs SCE.[21] A poly(pyrrole) layer was formed by the polymerization of pyrrole (0.02 M at pH = 1.0, HCl) using acidic 0.006 M of $FeCl_3 \cdot 6H_2O$ as initiator. After aging for 20 min, the solution was filtered through a fritted funnel keeping most of the black pyrrole. The doping of the Ppy layer is controlled by the oxidizing agent-to-pyrrole ratio. It has been characterized by the absorption spectrophotometry prior to filtration[22,23] which revealed an intense interband absorption band at 382 nm (3.25 eV) characteristic of a $\pi \rightarrow \pi^*$ transition of the π electrons in the highest occupied molecular orbitals and a weaker adsorption band at 460 nm (2.70 eV) attributed to the presence of short cationic conjugated segments.[23] The extent of doping was found to be time-dependent and was monitored spectroscopically by plotting the ratios of absorbances at 460 nm to 382 nm against time. Generally, solution aged for 20 min exhibited an absorption ratio of about 2.7, indicating that about 40% of the Ppy had been effectively doped.

Preparation of Poly(3-methylthiophene), PMeT. PMeT films were electrochemically synthesized. For deposition onto the pretreated ITO substrates an electrolytic medium consisting of $Li^+BF_4^-$(0.5 M) and monomeric 3-methylthiophene (0.4 M) in benzonitrile was used.[24] For deposition onto pretreated gold substrates an electrolytic bath containing tetrabutylammoniumtetrafluoroborate, $TBA^+ \cdot BF_4^-$ (0.1 M), and monomeric 3-methylthiophene (0.01 M) in HPLC acetonitrile was used.[25] Prior to use the monomeric 3-methylthiophene solution was degassed under vacuum below its boiling point for 20 min and then transferred to a drybox where the electrolytic bath had been prepared in a Schlenk flask. The degree of oxidation of PMeT was estimated to be 0.12 charge per monomer unit.[25b]

Deposition of the Ppy Layer onto the Pretreated Substrates. Ppy layers were deposited by repeated dipping of the pretreated substrate into the filtered Ppy solution, typically for a period of 2 min, and washing extensively with deionized water. The dipping and washing sequence was repeated until the desired thickness was reached. The dipping time was increased (by a factor of 10−15) when more qualitative filtration was performed without improving the stability of the resulting Ppy solution. In a typical procedure, precoated substrates were immersed into aged (typically for 20 min) and filtered Ppy solutions for two minutes for five times and washed by deionized water between each times. Such treatment led to 100−200 Å thick Ppy layers. The RMS value for the surface roughness of a 80 Å thick Ppy layer, deposited onto a precoated gold substrate, was determined to be 18 Å.

Deposition of the PMeT Layer onto the Pretreated Substrates. The deposition of a doped PMeT layer was carried out in a Schlenk flask electrochemically. A potential of 10 V was applied across the pretreated ITO working electrode (the substrate), a platinum counter electrode, and a silver reference electrode in the appropriate electrolytic medium under an argon atmosphere. A potential of 1.1 V was applied across the pretreated gold working electrode (the substrate), a platinum counter electrode, and a silver reference electrode in the appropriate electrolytic medium under an argon atmosphere. In both cases the film thickness was controlled by varying the amounts of charge responsible for the polymerization. Because the oxidation potential at which the polymerization of oligomers occurs is lower than that due to the conversion of the monomer, the obtained films were directly in a p-type conducting state as characterized by their deep blue color.[26]

Synthesis of CdSe Nanocrystals. CdSe nanoparticles were prepared by the published procedure.[27,28] Briefly, 0.0035 mol of dimethylcadmium was first added to 0.0025 mol of Se dissolved in 20 mL of trioctylphosphine (TOP) in an Ar-filled drybox. The mixture was transferred to a syringe and injected into pure melted trioctylphosphine oxide (TOPO), previously degassed under vacuum at 310−350 °C, under vigorous stirring at the same temperature and under argon (1 atm). Purification and size-selective precipitations were carried out three times in ethanol, followed by redispersion in butanol.[27] The synthesized nearly monodisperse suspension contained TOPO capped (hence the positive charge) CdSe nanocrystals of 35−37 Å in diameter, as deduced from visible spectroscopy and ellipsometric measurements.

Self-Assembly Procedure. Multilayers of CdSe nanocrystallites were prepared by using 1,6-hexanedithiol as anchoring molecule.[7,16] The layering procedure consisted of dipping successively the SCP covered pretreated substrate into (i) an aqueous 5 mM 1,6-hexanedithiol solution for at least 12 h and (ii) into a CdSe nanoparticle dispersion in butanol (approximately 4×10^{-3} M) for 7−8 h. The thiolated gold substrate was washed with deionized water for 20 s and then ethanol also for 20 s. After dipping in the CdSe suspension the substrate was thoroughly washed with butanol (30 s) and ethanol (20 s). In some cases, negatively charged organic (PSS) and inorganic (α-ZrP) polyelectrolytes were self-assembled onto the SCP covered pretreated substrate (Au/MEA/Ppy) prior to the self-assembly of CdSe. This self-assembly was accomplished by dipping the Au/MEA/Ppy film into a 0.02 M PSS solution (pH = 1.0), for 10 h, followed by washing with deionized water (20 s) and drying under an Ar gas stream, or a diluted colloidal suspension (6×10^{-4} M) of α-ZrP for 5 s, followed by a washing with deionized water (30 s) and ethanol (20 s) and drying via Ar gas. Ellipsometric measurements indicated that a PSS layer of 6.5 Å ± 2 Å and an α-ZrP film of 10 Å ± 1 Å (consistent with the value expected for a monolayer of sheet, thickness 6.5 Å) were formed onto Au/MEA/Ppy films. All the film-supported substrates were stored in air.

Results and Discussion

Strategy of Device Construction. Layer-by-layer assembly and self-assembly of a versatile rectifying device capable of undergoing a Zener breakdown has been the objective of the present work. Our interest has been prompted by the possibility of developing an ultrathin flat-panel-display screen based on a phosphor[29] whose electroluminescence can be triggered by "hot" electrons produced by the Zener breakdown at an p−n type

(21) (a) Kanazawa, K. K.; Diaz, A. F.; Geiss, R. H.; Gill, W. D.; Kwak, J. F.; Logan, J. A.; Rabolt, J. F.; Street, G. B. *J. Chem. Soc., Chem. Commun*. **1979**, 854. (b) Diaz, A. F.; Martinez, A.; Kanazawa, K. K. *J. Electroanal. Chem*. **1981**, *130*, 181. (c) Bull, R. A.; Fan, F. R.; Bard, A. J. *J. Electrochem. Soc*. **1982**, *129*, 1009.

(22) Brédas, J. L.; Scott, J. C.; Yakushi, K.; Street, G. B. *Phys. Rev. B* **1984**, *30*, 1023.

(23) Yakashi, K.; Lauchlan, L. J.; Clarke, T. C.; Street, G. B. *J. Chem. Phys*. **1983**, *79*, 4774.

(24) (a) Kaneto, K.; Yoshino, K.; Inuishi, Y. *Jpn. J. Appl. Phys*. **1983**, *22*, L567. (b) Kaneto, K.; Kohno, K.; Inuishi, Y. *J. Chem. Soc., Chem. Commun*. **1983**, 382.

(25) (a) Tourillon, G.; Garnier, F. *J. Electroanal. Chem*. **1982**, *135*, 173. (b) Waltman, R. J.; Bargon, J.; Diaz, A. F. *J. Phys. Chem*. **1983**, *87*, 1459. (c) Tourillon, G.; Garnier, F. *J. Electroanal. Chem*. **1984**, *161*, 51.

(26) Tourillon, G. In *Handbook of Conducting Polymers*; Skotheim, T. A., Ed.; Marcel Dekker: New York, 1986; pp 293−350.

(27) Murray, C. B.; Norris, D. J.; Bawendi, M. G. *J. Am. Chem. Soc*. **1993**, *115*, 8706.

(28) Hines, M. A.; Guyot-Sionnest, P. *J. Phys. Chem*. **1996**, *100*, 468.

(29) Rack, P. D.; Naman, A.; Holloway, P. H.; Sun, S.-S.; Tuenge, R. T. *Mater. Res. Soc. Bulletin* **1996**, *XXI*, 49.

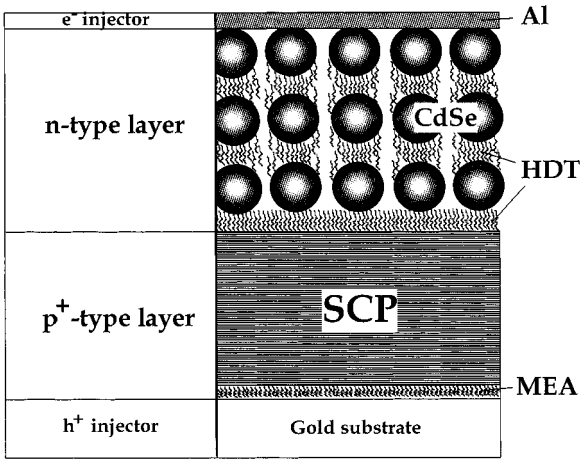

Figure 1. Fabrication of p^+-n junction by layer-by-layer assembly and self-assembly, capable of functioning as a rectifying device undergoing a Zener breakdown. The device consists of two layers: the first layer is a p-doped semiconductor polymer, SCP (polypyrrole, Ppy, for example), deposited onto a pretreated (by mercaptoethylamine hydrochloride, MEA) conducting substrate (gold, for example) which serves as the anode. The second layer is composed of n-type of semiconductor nanoparticles (cadmium selenide, CdSe, for example) and 1,6-hexanediol, HDT, layer-by-layer self-assembled onto the first layer and coated by a thin film of aluminum (Al) which serves as the cathode.

junction. The device fabricated consisted two layers. The first layer contained a p-doped semiconductor polymer, SCP (polypyrrole, Ppy, for example), of variable thickness, deposited onto a pretreated (by mercaptoethylamine hydrochloride, MEA) conducting substrate (gold, for example) which served as the anode. The second layer consisted of n-type of semiconductor nanoparticles (cadmium selenide, CdSe) and 1,6-hexanedithiol, HDT, layer-by-layer self-assembled onto the first layer and coated by a thin film of aluminum (Al) which served as the cathode (see Figure 1). Controlling the Zener breakdown by appropriate doping the SCP layer has been pivotal to our approach. Our design strategy has involved the selection of the most suitable SCP and semiconductor nanoparticles by considering their energy levels, the optimization of the composition and the thickness of each layer, and the doping of the SCP layer.

Selection of SCP and Semiconductor Nanoparticles. Components of the device have been selected by considering their charge injection energy levels. An appropriate matching must exist between the ionization potential (HOMO) of the p-type SCP and the anode, between the electron affinity of the n-type semiconductor nanoparticles and the cathode, and between the SCP and the semiconducting nanoparticles. The effect of thiolated molecules (1,6-hexanedithiol, HDT, and mercaptoethylamine, MEA) on the electronic characteristics of the device has been neglected because of the very high electron affinity and band gap of these molecules. Energy diagrams of the systems investigated in the present work is illustrated in Figure 2.

CdSe nanocrystallites have an electroaffinity of 3.00 eV[7,30] and a band gap of 2.10 eV[7] quite comparable to those of poly-(3-methylthiophene), PMeT (2.84 and 2.10 eV, respectively[31]). It is known that when PMeT is p-doped at less than 30%, the bipolaron levels appear inside the band gap at about 0.7 eV

(30) Colvin, V. L.; Alivisatos, A. P.; Tobin, J. G. *Phys. Rev. Lett.* **1991**, *66*, 2786.

(31) Yoshino, K.; Onoda, M.; Manda, Y.; Yokoyama, M. *Jpn. J. Appl. Phys.* **1988**, *27*, L1606.

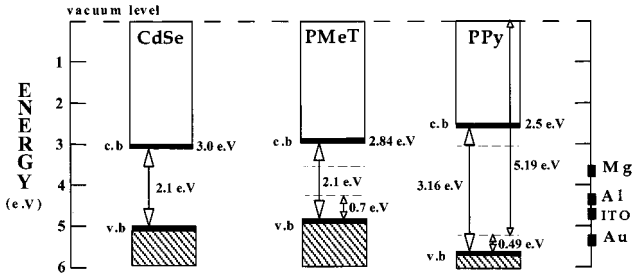

Figure 2. Schematic energy level diagram for a p^+-n junction consisting of a p-doped semiconductor polymer (poly(pyrrole), Ppy, or poly(3-methylthiophene), PMeT) and CdSe nanoparticles.

from the valence band and conduction band edges. In that case, the bipolaron level closer to the valence band edge participates in the activity of the p-junction when hole injection occurs in the vicinity of this level (i.e., for gold substrates, for example). The polaron level of Ppy, 5.19 eV (relative to the vacuum level), is at a range comparable to that required for exciton formation from CdSe; an energy difference of 2.19 eV separates the two levels of CdSe and Ppy; as compared to a difference of 1.94 eV between CdSe and PMeT (see Figure 2).

These considerations led us to focus our attention on two systems: Au/PMeT/$(HDT/CdSe)_3$ (Device A) and Au/Ppy/$(HDT/CdSe)_3$ (System B). Details on the composition of these two systems and on others examined are summarized in Table 1.

Optimization of the PMeT Layer. The electrochemical deposition of a semiconducting thin film onto a conductive substrate is expected to produce a very rough surface. Surface roughness was decreased by the use of such anchoring molecules as mercaptoethylamine, MEA (with Au substrate) and (4-aminobutyl)dimethylmethoxysilane (with ITO coated glass substrates). Surface roughness, evaluated by AFM, indicated a typical RMS value of 110 Å for an electrochemically deposited 500−600 Å thick film. The anchoring molecules, by virtue of providing a uniform monolayer coverage, also improved the homogeneity of the subsequent semiconductor nanoparticle layer.

Optimization of the Ppy Layer. Ppy binds irreversibly to the MEA-derivatized surface, presumably through nucleophilic attack of the amino group on the oxidized aromatic polymer. The Ppy solution contains positively charged oligomers, dispersed by electrostatic repulsions, and less doped oligomers, often referred to as black pyrrole, black-Ppy, which tend to aggregate on aging. Ppy solutions were always freshly prepared and used within a couple of hours. Filtration of the black Ppy and repeated washing were found to be necessary to obtain good quality Ppy films. Repeated washing of the substrates considerably enhanced the deposition rate for a given dipping time. The reformation of black Ppy after filtration slows down the kinetic of growth of the doped oligomers in the neighborhood of the substrate by a "screening effect". At a certain threshold, depending upon the pH and on the deposition time, the concentration of the aggregates became large enough for inducing an irreversible deposition onto the substrate and inhibiting further deposition of doped oligomers (Figure 3). TEM picture of a Ppy film, prepared by dipping the substrate into a Ppy solution for 20 min (and unwashed) taken on a derivatized copper grid, evidenced the presence of ellipsoidal particles of 500 ± 80 Å in height in good accord with values measurement by ellipsometry (630 Å $\pm$ 10 Å). At this stage, passivation of the surface reactivity was indirectly observed, both by visible spectroscopy and ellipsometry; attempts to deposit Ppy from

Table 1

initial derivatized substrate	type of interaction[a]		self-assembly	electro-chemistry	solvent(s)	thickness of one CdSe layer[b]	$V_{o.c.}$ (V)
	covalent binding	electrostatic interaction					
	between	between	Device A				
Au/PMeT/	$(PMeT/HDT)_1$		no	yes	ethanol		+1.0
Au/PMeT/HDT/	$(HDT/CdSe)_n$		yes	yes[c]	butanol	35 Å	+0.6[d]
							+1.2−1.4[e]
			Device B				
Au/MEA/Ppy/	$(Ppy/HDT)_1$		no[f]	yes	ethanol		+0.47
Au/MEA/Ppy/HDT/	$(HDT/CdSe)_n$		yes	yes	butanol	35 Å	+0.45
Au/MEA/PAH/		$(PAH/CdSe)_1$	no	no	water	20 Å[g,h]	
Au/MEA/Ppy/PSS/		$(PSS/CdSe)_1$	yes	no	water	25−26 Å[h]	
Au/MEA/Ppy/α-ZrP/		$(\alpha\text{-}ZrP/CdSe)_1$	yes	no	butanol	17−20 Å[h]	

[a] Interactions between the two outermost layers as indicated by the brackets. [b] The diameter of CdSe nanoclusters was about 37 Å. [c] Although CdSe can be deposited under a potential, the quality of the layer (uniformity, coverage) is not good enough. [d] Prior redoping. [e] After electrochemical redoping. [f] Including in acetonitrile, dioxane, *N*-methylformamide, THF, DMF, or neat HDT. [g] This layer is likely physisorbed and can be removed upon washing with water. [h] Further dipping in a capped CdSe butanol solution did not lead to additional deposition of CdSe nanoclusters.

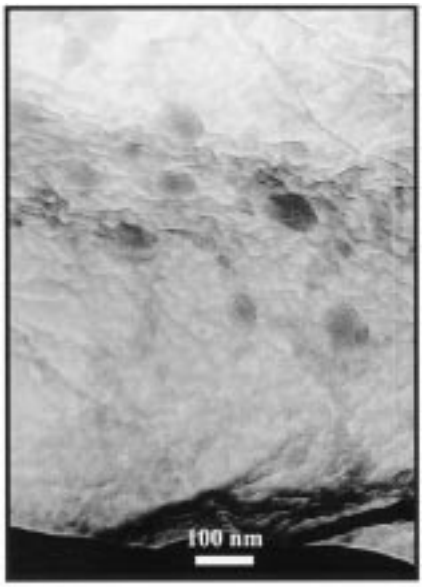

Figure 3. TEM image of a poly(pyrrole), Ppy, thin film (50 Å) prepared by dipping the substrate into a filtered solution of chemically p-doped Ppy for 20 min (without subsequent rinsing). The aggregates seen on the film are "black" pyrrole.

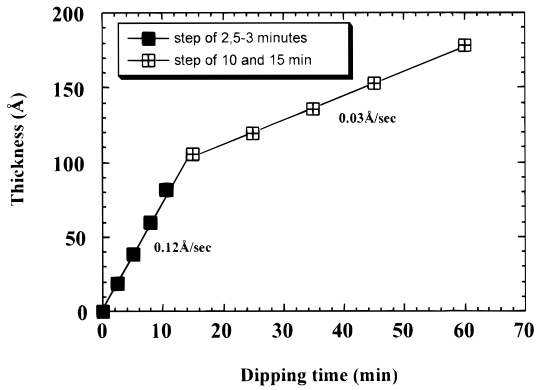

Figure 4. Correlation between the time of dipping of the pretreated (by mercaptoethylamine hydrochloride, MEA) gold substrate into filtered polypyrrole solution and the resulting thickness (Å) of a Ppy layer.

fresh solutions were unsuccessful. Attempts to lay down any other components (polyelectrolyte or HDT) onto the Ppy film also failed. This kind of passivation was attributed to the presence of big black Ppy aggregates (Figure 3). The thickness and the quality of the Ppy layers were found to depend on the frequency of the dipping and washing steps. Similarly, the rate of deposition was found to depend on the dipping time and the frequency of washing (see Figure 4); for example, it varied from 0.12 Å per s (2−3 min of dipping, washing after each dipping) to only 0.03 Å per s (10−15 min of dipping followed by washing).

Optimization of the Self-Assembly. Self-assembly onto the derivatized substrate was mediated by two types of interactions: covalent binding, in case of using thiolated molecules, and electrostatic interactions, in case of using organic and inorganic polyelectrolytes. Stability in common solvents and thicknesses of CdSe layers were routinely compared in order to select the most suitable procedure for self-assembly. Gold substrates were used for monitoring the thickness after each step by ellipsometry, while ITO coated glass and quartz substrates were chosen for studying the absorption properties of the different layers.

For ***Device A*** (see Table 1) alternating layers of HDT and CdSe were self-assembled onto an electrochemically deposited PMeT layer. Self-assembly of HDT onto TOPO-capped CdSe, resulted in the progressive displacement of the trioctylphosphine shell by covalently bonded 1,6-hexanethiol molecules (Figure 5). This self-assembly, on a derivatized gold substrate (Au/PMeT), was successfully repeated up to 10 sandwich layers (i.e., $Au/PMeT(HDT/CdSe)_{10}$). In the present work we limited our electrochemical studies to ***Device A*** which contained only three sequences of HDT/CdSe (i.e., $Au/PMeT(HDT/CdSe)_3$, see Table 1). Three sandwich layers of capped cadmium selenide, $(HDT/CdSe)_3$, self-assembled onto poly(phenyl−phenylene) has been reported to be sufficient for the detection of electroactivity.[7]

For ***Device B*** (see Table 1) alternating layers of HDT and CdSe were self-assembled onto a Ppy layer by taking advantage of the covalent binding of HDT to CdSe. To obtain an understanding of the interaction between HDT and the semiconducting polymer (Ppy) and between HDT and CdSe we surveyed the effect of the solvents on the anchoring reaction. Using an ethanolic solution as a solvent for HDT led to a complete dissolution of the ultrathin Ppy layer, after a contact time of 2−3 h only. However, depending on the concentration of HDT and contacting time, a monolayer of HDT could be anchored to the Ppy surface. The use of a nonprotic and polar solvent such acetonitrile or dioxane was found to inhibit interaction of HDT with the Ppy layer. Similarly, the use of

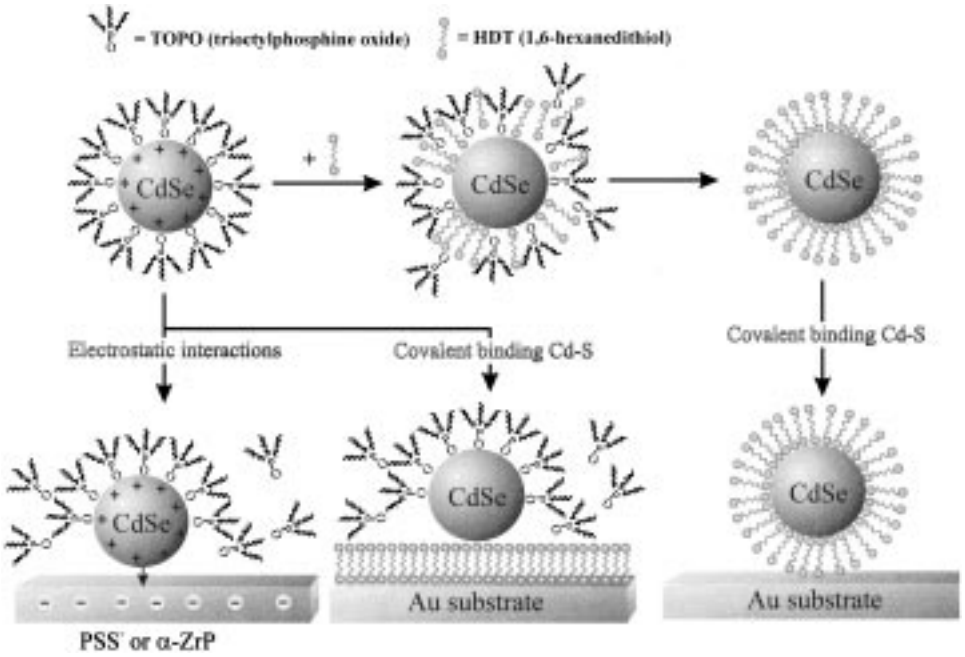

Figure 5. Simplified representation of the self-assembly involved in the layering of CdSe nanocrystallites, via electrostatic interactions (left) or covalent binding (right).

N-methylformamide, THF, and DMF resulted in insufficient binding of HDT. Using neat HDT also resulted in the complete dissolution of the polymer ultrathin layer. This result was somewhat unexpected in view of the well known formation of thiol monolayers on gold substrates in ethanol, acetonitrile, THF and DMSO.[32] HDT could however be attached to Ppy electrochemically (see below).

Additionally, alternating layers of polystyrene sulfonate, PSS (or α-ZrP), and CdSe were self-assembled onto a Ppy layer by taking advantage of attractive electrostatic interactions. In this approach we have been guided by the successful demonstration of ultrathin film formation between semiconductor nanoparticles and oppositely charged polyelectrolytes and surfactants by electrostatic interactions.[12a,15a]

Self-assembly by electrostatic interactions was investigated first by using positively charged polyallylamine hydrochloride, PAH, as the primer. Not surprisingly, dipping a derivatized gold substrate which had been coated by a 3−4 Å thick PAH layer (i.e., Au/MEA/PAH) into a CdSe dispersion for 15 h resulted in the physisorption of a 20 Å thick layer of semiconductor nanoparticles, easily removed by rinsing by ethanol.

Conversely, negatively charged PSS and α-ZrP could be self-assembled onto the positively charged Ppy film in the Au/MEA/Ppy system. Electrostatic attraction between Ppy and PSS (or α-ZrP) was found to be, in fact, so strong that even sonication in ethanol (20 min, in an ultrasonic cleaner) did not result in the separation (or exfoliation) of the self-assembled Au/MEA/Ppy/PSS or Au/MEA/Ppy/α-ZrP films. These two stable multilayers were used as substrates for the self-assembly of CdSe nanoparticles. The resulting mean thicknesses of the CdSe layer, determined by ellipsometry, were 25−26 Å (in Au/MEA/Ppy/PSS/CdSe) and 17−20 Å (in Au/MEA/Ppy/α-ZrP/CdSe), respectively. The principle of the electrostatic binding is depicted in Figure 5. Positively charged CdSe nanoparticles were self-assembled by immersing Au/MEA/Ppy/PSS or Au/MEA/Ppy/α-ZrP into an alcoholic dispersion of capped CdSe for approximately 15 h. However, in the Au/MEA/Ppy/PSS system the charge at the PSS interface, depending on the thickness and the level of doping of the Ppy layer, could be sufficiently neutralized to prevent further binding of CdSe nanoparticles. Interestingly, CdSe nanoparticles, self-assembled onto Au/MEA/Ppy/PSS, could not be derivatized by HDT. Contacting the Au/MEA/Ppy/PSS/CdSe film with HDT resulted in the quantitative release of CdSe nanoparticles, due to covalent bond formation (between HDT and CdSe). Attempts to sequentially self-assemble CdSe nanoparticles and α-ZrP onto Au/MEA/Ppy/α-ZrP did not succeed. α-ZrP was able to form a 12 Å thick layer on the top of Au/MEA/Ppy/α-ZrP/CdSe, but dipping the resulting film into a CdSe suspension (for 20 h) led to the formation of a layer characterized by a thickness of only 7−8 Å only. Evidently, capped CdSe nanoparticles poorly interacted with the second layer of α-ZrP, suggesting that the role of the Ppy layer is important in balancing the charges in these self-assembled systems.

Optical Properties and Photoluminescence of the Device Components. Poly(3-methyl thiophene). The p-doped PMeT film showed a strong absorption band with a maximum at 758 nm and a small shoulder at 470 nm (Figure 6). This absorption spectrum is comparable to that reported for polythiophene (interband transition at 420 nm and absorption above 600 nm due to the gap states[33]). The band at 760 nm was characteristic of a transition between the valence band and the bipolaron state located at about 1.6 eV above it.[26,34] Undoped films were characterized by a strong absorption at 506 nm, while broad band absorption centered at 352 nm (3.52 eV) indicated an overoxidized film with an important loss of conducting properties.

Poly(pyrrole). After layering, films of Ppy (150−200 Å) were characterized by an absorption band centered at 450−470 nm (2.75−2.64 eV) and a broad absorption in the range of 700−800 nm (and beyond) originating from the gap states and characteristic of a p-doping, respectively.[8]

(32) Bain, C. D.; Troughton, E. B.; Tao, Y.-T.; Evall, J.; Whitesides, G. M.; Nuzzo, R. G. *J. Am. Chem. Soc.* **1989**, *111*, 321.

(33) Kaneto, K.; Agawa, H.; Yoshino, K. *J. Appl. Phys.* **1987**, *61*, 1197.

(34) (a) Brédas, J. L.; Themans, B.; Andre, J. M. *Synthetic Metals* **1984**, *9*, 265. (b) Chung, T.-C.; Kaufman, J. H.; Heeger, A. J.; Wudl, F. *Phys. Rev. B* **1984**, *30*, 702.

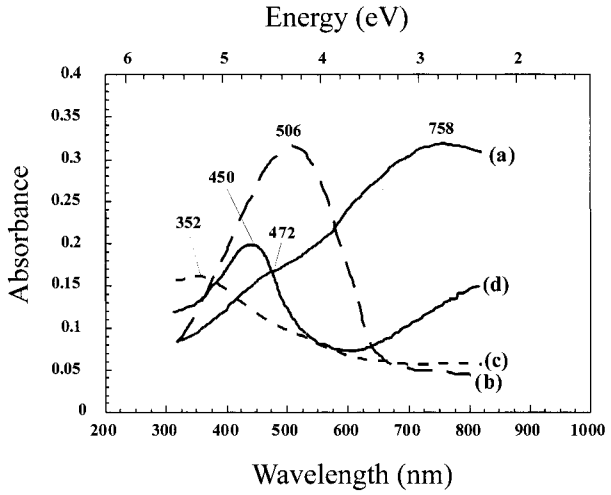

Figure 6. UV−visible absorbance of heavily p-doped (a); dedoped (b); and overoxidized poly(3-methylthiophene) films (c); and chemically p-doped 200 Å thick Ppy film (d).

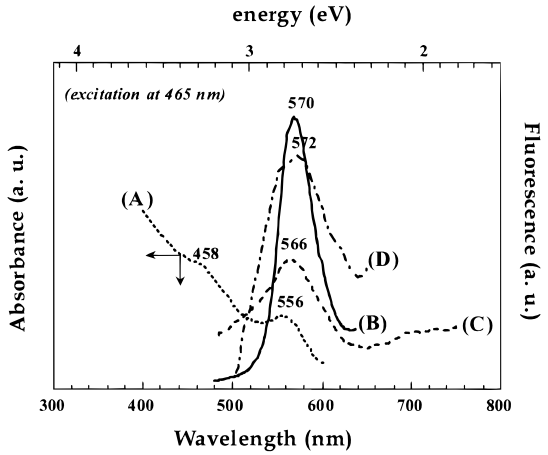

Figure 7. (A) = Visible absorption spectrum of CdSe nanoclusters dispersed in butanol; (B) = fluorescence spectrum of the same solution after excitation at 465 nm; (C) = emission spectrum collected for one monolayer of CdSe bound to a quartz substrate coated with pellicular α-ZrP; (D) = emission spectrum obtained after deposition of three sequences (HDT/CdSe) onto ITO substrate. It should be noted that the maximum emission band is almost exactly three times higher than the maximum measured in (C).

CdSe Nanoparticles. The TOPO capped CdSe nanoparticles dispersed in anhydrous butanol were optically characterized (Figure 7). The photoluminescence spectrum, obtained by excitation at 465 nm, manifested itself in a narrow emission band at 570 nm, in accord with previously published data,[27] and had a quantum yield of 5% (calculated by using the emission of Rhodamine B as a reference). Photoluminescence spectra of CdSe nanoparticles were routinely used to monitor the efficiency of the self-assembly in the different systems, particularly that based on electrostatic interactions. The normalized emission spectrum obtained for one CdSe monolayer adsorbed onto the quartz/AMS/Ppy(20 Å)/α-ZrP(10 Å) film exhibited a band at 566 nm with a third of the intensity of that measured at 572 nm for the ITO/AMS/Ppy(80 Å)/(HDT/CdSe)$_3$, indicating that the coverage resulting from electrostatic interactions is comparable to that observed for dithiols for one monolayer of CdSe. The absorption spectrum of quartz/AMS/Ppy(20 Å)/(HDT/CdSe)$_n$ with n = 1, 2, or 3 was found to red shift with respect to a single CdSe monolayer (from 543 to 548 nm, Figure 8).

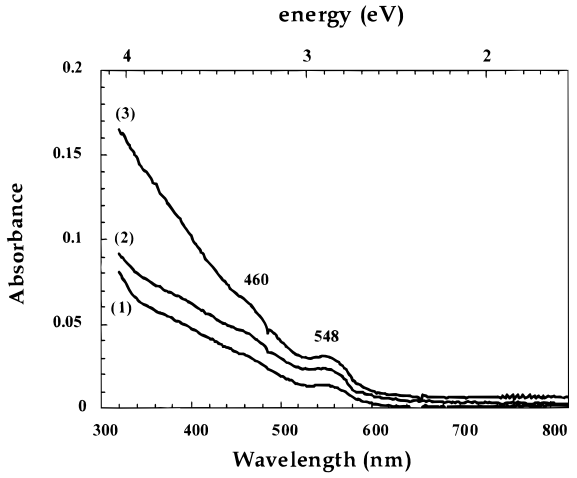

Figure 8. UV−visible spectra of CdSe nanocrystallites (diameter ∼ 35 Å) obtained for ***Device B*** [(ITO/anchoring agent (4-aminobutyldimethoxysilane, AMS)/Ppy(20 Å)/(HDT/(CdSe)$_3$] showing the sequential absorption increase of a first (1), second (2), and third (3) layer of CdSe.

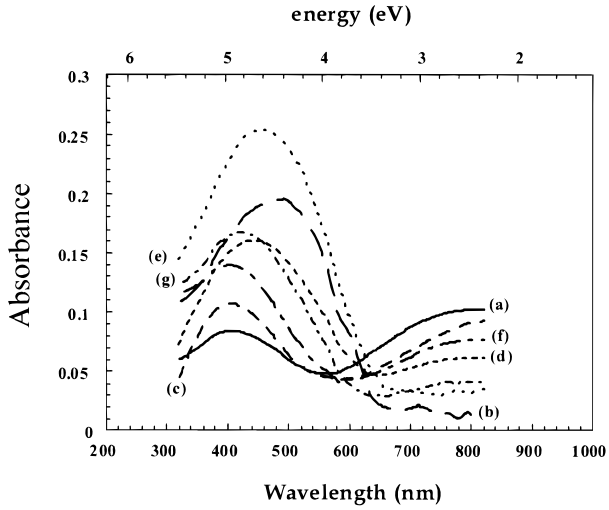

Figure 9. UV−visible spectra recorded after each deposition process of a device formed by a sequence ITO/PMeT(film)/(HDT/CdSe)$_3$/HDT: (a) = after electrochemical deposition of HDT onto PMeT; (b) = followed by chemical deposition of CdSe; (c) = a redoping at +1.4 V vs Ag/Ag$^+$ in anhydrous ethanol (without adding electrolytes); (d) = a second electrochemical deposition of HDT; (e) = a chemical deposition of CdSe; (f) = a redoping; and (g) = a final electrochemical deposition of HDT.

Optical Properties of Doped and Undoped SCP Films. The marked electronic transition which accompanies doping and dedoping of PMeT films was used to characterize and monitor the optimization of the layering and of the self-assembly by absorption spectrophotometry. Self-assembling of negatively charged polymers (PSS) or inorganic sheets (α-ZrP) on the top of a ITO/AMS/Ppy film resulted in a dedoping, as indicated by the appearance of a strong red color and an absorption band at 506 nm. However, when a monolayer of HDT was deposited under an adequate potential (i.e., +1.4 V vs Ag/Ag$^+$), the film could maintain the initial doping, as demonstrated by optical spectroscopy (Figure 9).

Immersion of the ITO/PMeT/HDT film in an alcoholic dispersion of CdSe resulted in quantitative dedoping; as indicated by the appearance of the absorption band at 508 nm with an onset close to 600 nm (see curve a in Figure 9). The redoping was affected by reimmersion of the Au/PMeT/(HDT/

$CdSe)_n$ or the ITO/PMeT/$(HDT/CdSe)_n$ films in a HDT solution for 10−15 min (depending on the nature of the substrate). Redoping was accomplished by BF_4^- ions trapped or still remaining in the polymer. Alternatively, redoping was carried out after each step of CdSe nanoparticle self-assembly, by placing the film into an electrolytic bath which contained 0.05 M $TBA^+ \cdot BF_4^-$ in acetonitrile (see below). Redoping was monitored by absorption spectrophotometry by following the growth of the band at 400−430 nm and the appearance of a new band with a maximum at 800 nm (1.55 eV), characteristic for p-type doping (see curves c and f in Figure 9). The blue-shift of the absorption expected for an undoped ***Device A*** appeared both after derivatization of the polymer thin ***Device A*** and the CdSe monolayer formation when electrochemical method is used and increased after every electrochemical operation (see Figure 9). These films exhibited an open circuit voltage of only +0.6 V, indicating a partial loss of doping of PMeT. Indeed, the formation of shorter polymeric chains has been reported to be responsible for an increase in the effective value of the band gap.[35] Based upon the observed shift of the maximum absorption of the HOMO−LUMO transition (from 472 nm for a p-doped PMeT film to 420 nm for the ITO/AMS/PMeT/HDT film), we can estimate that the band gap increases about 0.3−0.4 eV after a complete electrochemical process leading to the deposition of three monolayers of CdSe. It has been reported that an overoxidation of the polymer occurs around a voltage of +1.8 V (vs Ag/Ag^+).[36] Overoxidation at these very positive potentials causes nucleophilic attack of water on the polymer and results in the formation of hydroxyl, carbonyl, quinone, and carboxylic groups.[37] These reactions also cause C−C bond cleavage and other structural defects, which reduce the conjugation length of the polymer. An increase in band gap is therefore indicative of shorter conjugation length.[38] This phenomenon was clearly observed both when an overpotential of +2.5 V or a potential of +1.4 V vs Ag/Ag^+ was applied to the ITO/AMS/PMeT$(HDT/CdSe)_n$ films. However a certain reversibility in the degradation of the polymer could still be evidenced on applying a potential of +1.4 V. This effect was visualized by following the shift of the absorption band located in the 400−500 nm region, depending on the level of doping. Indeed, electrochemical deposition of a first HDT layer onto PMeT was characterized by a band centered at 404 nm, which after deposition of a second and third layer of CdSe shifted to 445 and 420 nm, respectively. Figure 9 presents the evolution of the maximum absorption depending on the number of electrochemical or self-assembling operations.

The position of the absorption maximum was observed to correlate well with the extent of redoping of the ITO/AMS/PMeT$(HDT/CdSe)_n$ films (See Figure 9). Ratios of absorption maximum to absorbance ([λ(nm)]:[absorbance]) against the number of layers deposited (or self-assembled) provided an accurate appraisal of the efficiency of the redoping (Figure 10). This ratio increased after every redoping for a given sequence, but the ability for the device to be redoped decreased continuously with the number of sequences, indicating that the electronic properties of the polymer were irreversibly modified by an overoxidation reaction still occurring at a potential as low as +1.4 V. Alternatively, the counteranions, still trapped into the polymer network, became progressively released. In fact, a final redoping at the same potential in an electrolytic bath of 0.1 M $TBA^+ \cdot BF_4^-$ led to a quantitative redoping, with undoped domains characterized by an absorption band centered at 401 nm (compared to 420 nm prior redoping), demonstrating that both of these effects need to be considered.

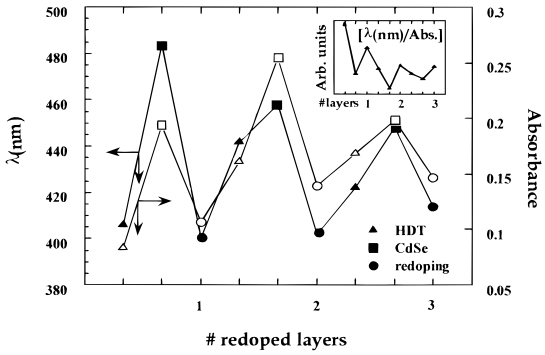

Figure 10. Comparisons between the wavelengths of the undoped domain in PMeT films and the corresponding absorbance as a function of the number of repeated sequences: derivatizing layer (HDT)/CdSe/redoping.

Control of the Doping. ***Device A.*** Once poly(3-methylthiophene) film was electrochemically deposited onto a gold or ITO substrate, contacting it with an alcoholic solution of HDT or CdSe resulted in a partial loss of the doping. This dedoping was alleviated by keeping the substrate (Au/PMeT) at a positive potential during the deposition of HDT or CdSe. Alternatively, a positive potential was applied after the formation of the HDT or CdSe monolayer. Application of a positive potential for several hours resulted in the dissolution of the PMeT film; therefore, potentials were applied only for a period necessary for redoping (typically for 20 min). The time duration of the potential applied depended on the thickness of the polymer film. Application of 2.5 V resulted in recovery of the initial level of doping of the Au/PMeT/HDT/CdSe film, characterized by an open-circuit voltage of 1.4 V.

Since the binding of HDT occurs by an oxidation reaction, dedoping of the Au/PMeT/HDT/CdSe film is the consequence of reduction. In any event, a p-doped PMeT film cannot be stable in an alcoholic medium because its oxidation potential (+1 V) lies near to the saturation potential of the ***Device A*** and promotes further reduction and dedoping. To control both the grafting of HDT and the doping of the film, the substrate contacted with a HDT solution was always kept at a positive potential. By applying a positive voltage, HDT was expected to bind rapidly and without causing any dedoping. A 1.4 V potential applied for at least 15−20 min resulted in the formation of a thiolated layer with a characteristic thickness of 12−13 Å when grafting on a gold substrate (whereas 15−20 h were necessary for anchoring the same layer in the absence of an applied potential). Similarly, a bias voltage was applied for comparable time duration in the case of a gold or ITO substrate having a polymer layer on the top in order to prevent quantitative dissolving of this layer. Electrochemical deposition of a CdSe layer did not improve the quality of the resulting monolayer (a marked inhomogeneity of the film was observed from the contact point of the electrode to the furthest area) nor the time necessary to obtain it. As a consequence, a typical procedure consisted of an electrochemical deposition of the anchoring molecule (HDT) followed by the immersion of the Au/PMeT/HDT/film into a CdSe dispersion for at least 2 h. Parallel with formation of the anchoring layer partial redoping occurred (see above).

In most cases a potential of +1.4 V was preferentially chosen in order to avoid the application of an overpotential. This

(35) Hoffmann, R. In *Solids and Surfaces: a Chemist's View of Bonding in Extended Structures*; VCH: New York, 1988.
(36) Krische, B.; Zagorska, M. *Synthetic Metals* **1989**, *28*, C257.
(37) Novák, P.; Müller, K.; Santhanam, K. S. V.; Haas, O. *Chem. Rev.* **1997**, *97*, 207.
(38) Brédas, J. L.; Street, G. B. *Acc. Chem. Res.* **1985**, *18*, 309.

Table 2

systems	medium	contacting time (min) at +2.5 V vs Ag/Ag^+	$V_{o.c.}$ (V)	absorbances[a] at 472 nm	absorbances[a] at 800 nm	ratio Abs(800)/Abs(472)
ITO/AMS/Ppy(50 Å)	neat EtOH	0	+0.55[b]	0.0438	0.0398	0.91
		10	+0.51	0.0308	0.0289	0.94
		20	+0.50	0.0094	0.0117	0.92
ITO/AMS/Ppy(35 Å)	5 mM HDT ethanolic solution	0	+0.57[b]	0.0316	0.0293	0.93
		10	+0.46	0.0315	0.0200	0.63
		20	+0.47	0.0308	0.0200	0.65
		50	+0.46	0.0293	0.0182	0.62

[a] A maximum of absorbance was observed at 472 nm in all cases, while a broad absorption band, characteristic of p-doping, appeared centered beyond 820 nm and has been arbitrarily monitored at 800 nm. [b] These values have been measured in both cases immediately after depositing the Ppy film and in neat EtOH.

potential was applied after each deposition step of a CdSe nanoparticle layer until an open potential circuit voltage of +1.2 V was achieved (typically after 15 min) in an acetonitrile doping solution containing 0.05 M $TBA^+ \cdot BF_4^-$. Nevertheless an almost complete redoping of the Au/PMeT/$(HDT/CdSe)_3$ films could be accomplished by the application of +2.5 V overpotential in the same medium for 80 s. Longer application times caused irreversible damage of the polymer film, with a loss of electroactivity, as evidenced by the presence of an absorption band at 352 nm (characteristic for an overoxidized film see curve c in Figure 6). It should be noted that these two procedures of redoping did not lead to detectable differences in the electroactivity of the full device.

Device B. A chemically p-doped Ppy layer in the Au/MEA/Ppy/HDT films also underwent dedoping during the self-assembly of HDT. To prevent both the dedoping and the dissolution of the polymer by long contacting time in this solution, the anchoring layer was electrochemically deposited at a constant potential of +2.5 V for 15 min. This, typically led to the formation of an 11 Å thick HDT layer and an open circuit voltage of +0.47 V demonstrating that the Ppy layer remained in a p-doped state. It has been reported that a Ppy film undergoes overpotential at potential more positive than +0.65 V vs Ag/Ag^+ in water.[39] To quantify the effect of the applied anodic potential on self-assembled Ppy layer, a 35−50 Å film was prepared onto an ITO/AMS substrate. The degree of oxidation of the polymer was monitored by means of UV−visible spectroscopy, while holding the potential at +2.5 V vs Ag/Ag^+ and contacting the surface with neat ethanol or with an ethanol−HDT electrolyte solution. From the time-dependent absorbance data (Table 2), it is apparent that the Ppy film is desorbed completely without overoxidation or dedoping in ethanol solutions that contained no HDT. The film remained doped while dissolving, as deduced from the values of $V_{o.c.}$ and the almost constant absorption ratio of 800 nm/472 nm. In the presence of HDT, however, both the open circuit voltage and the absorption ratio of 800 nm/472 nm decreased initially with time and then became constant, indicating that partial dedoping occurred. It is known that the rate of overoxidation of Ppy increases significantly in the presence of nucleophiles.[40,41] In the present case, it appears that HDT reacts promptly at the surface of the Ppy film, forming a passive layer that prevents further oxidation or dedoping from occurring. This reaction corresponds to a Michael addition of a nucleophile, generally an amine,[42] thiol in our case, to a conjugated double bond system, such as quinones produced during the overoxidation. Since the doping level of the Ppy layer was still high after the reaction with HDT, redoping was not attempted. In our study, Ppy films were about 10 times less rough than the electrochemically deposited PMeT films. Concomitantly, Ppy films were more stable and compact than their PMeT counterparts. Subsequent contact of the Au/MEA/Ppy/HDT films with CdSe suspension led to the deposition of a semiconducting monolayer of nanoparticles ($V_{o.c.}$ = 0.45 V) with a high level of coverage. The assembling procedure is schematically described in Figure 11. The relation between the absorption of CdSe nanoparticles at 448 nm and the number of sequences $(HDT/CdSe)_n$ deposited onto a thin layer of Ppy (20 Å) is illustrated in Figure 8. It can be seen that the first HDT/CdSe bilayer exhibits a more intense absorption than any of the subsequent bilayers, indicating the more dense coverage of the Ppy polymer than the CdSe nanocrystalline layer by HDT.

X-ray Photoelectron Spectroscopy. XPS spectroscopy was performed on two aged multilayer systems (stored 20 months in air): AMS/Ppy(20 Å)/$(HDT/CdSe)_3$/HDT, ***Device A***, and AMS/PMeT(500 Å)/$(HDT/CdSe)_1$/HDT, film B. Both films exhibited peaks corresponding to Cd, Se, S, C, O, and Sn. Importantly, no phosphorus peaks were detected, confirming the effective replacement of the TOPO by HDT on the CdSe nanoparticles during the self-assembly. By analyzing the Se 3d peaks region, it was found that a partial oxidation of Se occurred in both cases. In ***Device B***, peaks at 53.7 and 58.4 eV were assigned to the 3d level of Se atoms in CdSe and SeO_2, respectively (Figure 12). On this basis, an approximate curve fit to the Se 3d envelope for ***Device B*** gave a (selenide)/(selenium oxide) ratio of about 6/1. This value lies in the range of oxidation level expected for TOPO-capped CdSe nanocrystallites laid down onto HDT-derivatized gold substrate[43] upon exposure to air for 1 day and demonstrates the long-term stability of our multilayers. A close-up survey in the domain of Cd 3d revealed the presence of two peaks originating from levels 5/2 and 3/2. No cadmium oxide[44] was detected in this domain, confirming the crucial and stable bonding of thiols with Cd atoms. Nitrogen was not clearly identified in both films. In ***Device A***, a close-up survey in the binding energy region expected for N 1s did not show a peak at 401 eV as expected for doped poly(pyrrole).[44] This is probably due to the low sensitivity of N relative to Cd. It should be also noticed that some other elements, such as Si from AMS and In from the substrate itself, were also not detected, while obviously present.

(39) (a) Lewis, T. W.; Wallace, G. G.; Kim, C. Y.; Kim, D. Y. *Synthetic Metals* **1997**, *84*, 403. (b) Mostany, J.; Scharifker, B. R. *Synthetic Metals* **1997**, *87*, 179.

(40) (a) Novák, P.; Vielstich, W. *J. Electrochem. Soc.* **1990**, *137*, 1036 and 1681. (b) Schlenoff, J. B.; Xu, H. *J. Electrochem. Soc.* **1992**, *139*, 2397.

(41) (a) Beck, F.; Braun, P.; Oberst, M. *Ber. Bunsen-Ges. Phys. Chem.* **1987**, *91*, 967. (b) Novák, P.; Rasch, B.; Vielstich, W. *J. Electrochem. Soc.* **1991**, *138*, 3300.

(42) Deinhammer, R. S.; Ho, M.; Anderegg, J. W.; Porter, M. D. *Langmuir* **1994**, *10*, 1306.

(43) Bowen Katari, J. E.; Colvin, V. L.; Alivisatos, A. P. *J. Phys. Chem.* **1994**, *98*, 4109.

(44) Beadle, P. M.; Armes, S. P.; Greaves, S. J.; Watts, J. F. *Langmuir* **1996**, *12*, 1784.

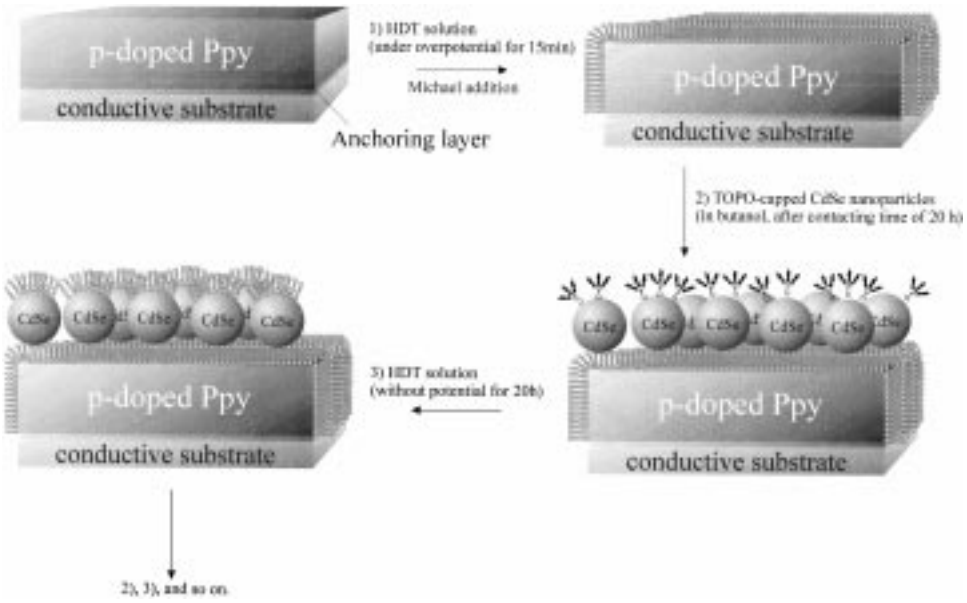

Figure 11. Schematic representation of the derivatization of a Ppy layer under overpotential in alcoholic solution of 1,6-hexanedithiol (HDT), followed by the chemical deposition of (CdSe/HDT) sequences.

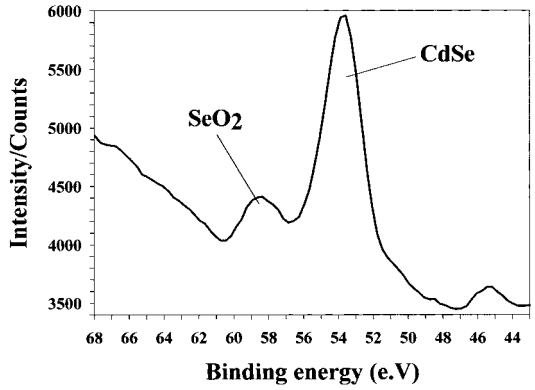

Figure 12. Close-up XPS survey spectra of Se-3d core for the system AMS/PMeT(500 Å)/(HDT/CdSe)$_1$/HDT, ***Device B***, after storage in air for 20 months. The SeO_2/CdSe = 1:6 ratio indicates the long term stability of ***Device B***.

Fitting parameters used in curve fits of the Se 3s/S 2s envelope were different for both samples; a shift of 0.6 e.V was measured between the compared S 2s envelopes, indicating that sulfur atoms were likely surrounded by two different environments in these two systems; indeed, in ***Device A***, only HDT was present, while thiophene units were largely predominant relative to HDT in ***Device B***.

i*−*V* Characteristics.** Electrical properties of the junctions, particularly those relating to Zener-breakdown, of ***Device A and ***Device B*** were characterized by current (*i*) voltage (*V*) measurements. The Zener breakdown was generally registered from freshly assembled films and was observed even after 1 week of standing, substantiating the good stability of the p^+-type layer. However, a systematic investigation of the device properties with respect to aging was not carried out. Injection of charges—holes and electrons—is believed to occur mainly by tunneling through the interfaces between the electrodes and the hole or electron conductors.[45] The tunneling mechanism can be expressed by the Fowler−Nordheim equation which describes the field emission tunneling current, *I*, as a function of the bias voltage[46]

$$I = V^2 \exp(-\beta d/V) \quad (1)$$

where *d* is the thickness of the device sandwiched between the electrodes. Plotting eq 1 logarithmically led to a good straight line (Figure 13) which permitted the fitting of the forward branch of the Fowler−Nordheim equation (see below). If a triangular barrier is assumed to govern the tunneling at the interfaces, the value of the constant β can be deduced from the following relation[47]

$$\beta = \frac{4\sqrt{2m^*}\phi^{3/2}}{3eh} \quad (2)$$

where β has the dimensions of electric field, and is related to a "critical field" for junction breakdown. The terms ϕ refers to the barrier height and m^* the carrier effective mass. *i*−*V* characteristics present two branches, in forward and reverse direction (Figures 14 and 15). In the reverse direction, the increase of current measured is very abrupt and do not follow neither a Schottky nor a Fowler−Nordheim law. Such a behavior has been observed for an asymmetric abrupt junction like p^+−n.[48] In our case, the level of doping inside the polymer is electrochemically or chemically promoted to a much higher value than that exist in the CdSe layer. This behavior is characteristic for the Zener breakdown and appears in a p−n junction in which the level of doping is strongly different,[48] i.e., p^+−n junction in the systems (***Device A*** and ***B***) examined here. Interestingly, when a PMeT layer was not subjected to redoping (i.e., the multilayer assembly was prepared without the supply of an electrochemical procedure), the breakdown was not observed.

At a Zener junction, the electric field is maximum at the interface between the p-and n-type material and varies as

(45) Parker, I. D. *J. Appl. Phys.* **1994**, *75*, 1656.

(46) Fowler, R. H.; Nordheim, L. *Proc. R. Soc. London Ser. A* **1928**, *119*, 173.

(47) Sze, S. M. In *Physics of Semiconductor Devices*; Wiley: New York, 1981.

(48) Mathieu, H. In *Physique des Semiconducteurs et des Composants Electroniques*; Masson, 1996; p147.

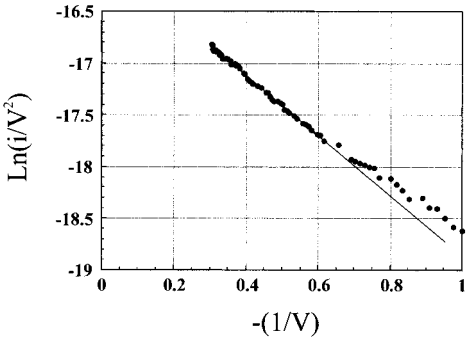

Figure 13. Fowler−Nordheim plot calculated from the i-*V* characteristics of the system Au/p-doped PMeT film/$(HDT/CdSe)_3$/(Al_2O_3)-Al in the forward direction. The *R*-value of the straight line is 0.998.

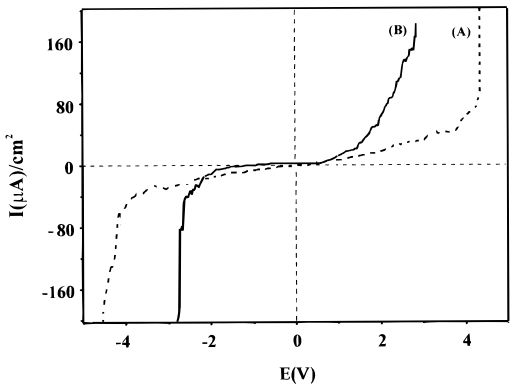

Figure 14. *i*−*V* characteristics measured for an Au/p-doped PMeT film/(Al_2O_3)-Al (A) and for an Au/p-doped PMeT film/$(HDT/CdSe)_3$/(Al_2O_3)-Al (B). The contact pad area was 2.5 cm^2.

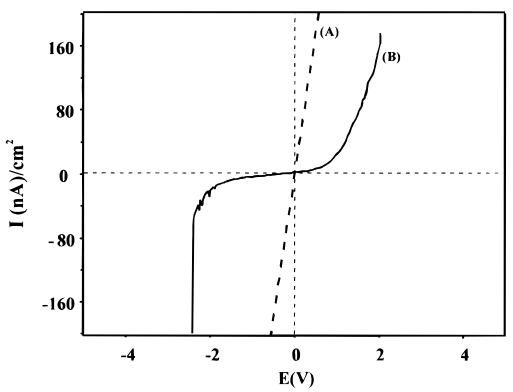

Figure 15. *i*−*V* characteristic obtained for (A) a sequence Au/Ppy-(∼100 Å)/(Al_2O_3)-Al and (B) a sequence Au/Ppy(∼100 Å)/$(HDT/CdSe)_3$/(Al_2O_3)-Al. The contact pad area was 2.5 cm^2.

$$E_o = \frac{eN_d W_n}{\epsilon} \quad \text{with} \quad W_n = \left(\frac{2\epsilon}{eN_d}(V_d + V_r)\right)^{1/2} \qquad (3)$$

where N_d is the donor density, W_n the length of the space charge layer, V_d is the difference of potential between the two regions, V_r is the reverse voltage. Thus, for $V_r = V_d$

$$E_o = 2\left(\frac{eN_d}{\epsilon}\right)^{1/2} \cdot V_r^{1/2} \qquad (4)$$

An electric force is promoted by the electric field E_o until the binding forces between "hot" electrons and nuclei are overcome, thus, the electrons of the valence band of the p-type region are released toward unoccupied states of the conduction band of the n-type region. The material becomes conductor and the voltage V_r readily stabilizes. The limit of V_r is depending upon both the width of the depletion layer and upon the levels of doping in the semiconductor. The limit observed for the reverse voltage is also called the Zener voltage V_z. The pairs hole-electron created by ionization are drained off by the electric field and generate an important reverse current. Electrons are directly emitted, by tunneling through the space charge layer, from the valence band to the conduction band. The voltage cannot increase beyond V_z, leading to the i-*V* characteristics reported in Figures 14 and 15. Typically, this effect is observed for heavily doped asymmetric p−n junction, having a very narrow space charge layer (∼ 500 Å) for V_z below five volts.[48]

The Zener breakdown should appear once a potential is reached which corresponds to that of the difference between the conduction band edge of CdSe and the valence band edge of the polymer. According to the energy level diagram sketched in Figure 2, this difference is between 2.3 and 2.4 eV at the PMeT/CdSe junction and about 2.66 eV at the Ppy/CdSe junction. It is observed that the breakdown occurs at about −2.5 and −2.3 V for PMeT and Ppy, respectively. Thus, the energy required for inducing a reverse current is in a fair agreement with the minimum energy to be applied by considering Figure 2, indicating that $V_d \approx V_r$ (eq 4) with the Zener breakdown taking place owing to the high density of donors N_d in the polymer film. However, the influence of the presence of polaron states between the donor and acceptor levels of the Zener junction is not quantified by eq 3, for example, the distance separating the polaron band from the valence band edge. It can be assumed that the presence of a polaron band close to the valence band might assist in the accommodation of extra-positive charges thus favoring the departure of electrons toward CdSe nanoparticles as expected if the breakdown occurs at a potential close to what we predict from the energy level diagram. This result is quite interesting and should allow further control of such a Zener breakdown by manipulating the nature of the SCP layer. The i-*V* characteristics observed for the junction Au/PMeT/Al_2O_3−Al (see curve A in Figure 14) is symmetric and can possibly be interpreted in terms of the ability for the polymer to accept both negative and positive polarons; this phenomenon has been previously observed for a poly(3-octylthiophene) thin layer sandwiched between ITO and Al electrodes.[33,49] However, there is still a slight ohmic behavior between the rectifying branches, possibly related to the direct contact with an oxidizing metal and its superficial oxide layer, as observed for the junction Au/Ppy/(Al_2O_3)-Al.[50]

Further assembly of several sequences of HDT/CdSe onto Au/PMeT/HDT/CdSe (***Device A***) and Au/MEA/Ppy/HDT/CdSe (***Device B***) demonstrates, that the presence of CdSe determines the i-*V* curves, with characteristics indicating, unambiguously, that a p^+−n junction has been formed. In the forward direction, the increase of current follows the Nordheim−Fowler equation whatever the nature of the SCP. Figure 13 shows the NF plot obtained in the case of a junction consisting in Au/PMeT(∼800 Å)/$(HDT/CdSe)_3$/(Al_2O_3)-Al. An expected Fowler−Nordheim behavior was observed above 1.5 V in the forward direction, with a noticeable deviation below this value. The barrier heights to the tunneling are low, comprised between 0.025 and 0.05 eV, depending on the polymer used, in the range of energy expected for a thermoionic formation of carriers; however, no matching with the Schottky equation was obtained. It should be noted that eq 2 is deduced from the flux of carriers by

(49) Garten, F.; Schlatmann, A. R.; Gill, R. E.; Vrijmoeth, J.; Klapwijk, T. M.; Hadziioannou, G. *Appl. Phys. Lett*. **1995**, *66*, 2540−2542.
(50) Inganäs, O.; Lundström, I. *Synthetic Metals* **1984/85**, *10*, 5.

considering an approximate expression for the tunneling probability of a triangular barrier.[51] Usually, the barrier height is in the order of 0.1 eV, and this approximation is no longer accurate at room temperature. The expression for the tunneling current requires an additional temperature-dependent term.[51] Such a corrected equation explains the observed deviation from the FN law at small applied fields[52] and might also account for the present deviation (Figure 13). Additionally, the applicability of this equation remains valid as long as $\beta < [(1/k_BT) - (1/\phi)]$. If this condition is not fulfilled, thermoionic emission dominates the current injection.

Previous studies on related organic−inorganic p−n junctions generally involved PMeT and bulk CdS,[53] Ppy and bulk CdS,[54] PPV or hole transporting layer and CdSe quantum dots,[7,15] and PPV and CdS films.[55] To the best of our knowledge, in none of these cases, a Zener diode behavior was mentioned. Bulk CdS was used with a SCP for promoting photovoltaic properties; the valence band edge of p-doped PMeT or Ppy was lying in vicinity of the conduction band edge of CdS (4.5 eV vs vacuum[53c]); in that case a metallic-like SCP layer was deposited onto a CdS crystalline thick layer leading to a semiconductor-metal Schottky-type junction at forward bias. Observation of a Zener breakdown in a device exhibiting good photovoltaic properties is highly unlikely since the close vicinity of the valence band of the SCP to the conduction band of the inorganic semiconductor should result in charge scavenging under reverse bias.

The electroluminescent devices based on CdSe quantum dots and polymeric hole transporting materials exhibit a more complicated thickness dependent $i-V$ characteristics.[14b] The current, on using poly(vinylcarbazole) and an oxadiazole derivative, was found to be dependent on the strength of the electric field, and a symmetrical $i-V$ curve was observed.[14b] It should be noted that these devices were found to be both non-Ohmic and nonrectifying in the classical sense. On the other hand, Colvin et al. reported a Schottky-like behavior at forward bias for a PPV/$(HDT/CdSe)_n$ system[7] with $i-V$ curves independent of the sample thickness.[56] In this case, the charge injection was dominated by the metal-nanocrystal junction. More recently, a CdS layer was deposited by wet chemical processing onto a PPV layer and submitted to annealing, to stimulate the electroluminescence by improving the electron injection into the device.[55] With the PPV-based devices, the effect of chemically depositing CdSe quantum dots or a CdS film on the final doping of the SCP was not evaluated, and the method of deposition of HDT onto PPV was not clearly stated.[7,15,56] Furthermore, the spin-coated PPV film was obtained by the thermal treatment of the PPV-precursor in a reducing atmosphere, which leads to undoped PPV.[56] Under reverse bias, due to the blocking nature of the electrodes and the presence of a p−n junction, no current rectification is expected. It is likely that depositing an n-type semiconducting layer onto a SCP layer strongly affects the conducting properties of the p-type layer, as it is demonstrated in this study. It is therefore essential to maintain an appreciable level of doping in the SCP layer by an appropriate chemical surface passivation for promoting a Zener diode behavior. The degree of organization of the polymer also influences the quality of the interface, as it can be seen for systems in which the Ppy and PMeT layers had been deposited by two different approaches (see above).

Conclusion

Details have been provided in this paper on the assembly and self-assembly of ultrathin functioning p−n junction based devices, capable for rectification and Zener breakdown. The main interest in Zener breakdown is to produce "hot" electrons in the n-type layer which could be used, for instance, for stimulating the luminescence in a phosphor and hence to provide a route to bimodal electroluminescence, with two distinguishable emissions depending on the potential direction. Further works should be devoted to the synthesis and stabilization of nanocrystalline phosphors (i.e., earth rare doped II−VI semiconductors) into similar devices. Most significantly, however, the present work has demonstrated the versatility and power of the self-assembly chemistry approach in nanostructuring advanced electronic devices.

Acknowledgment. We thank the National Science Foundation (CHE-9529202) for support of this research. Instrumentation for AFM experiments was provided by National Science Foundation Grant CHE-9626326. T.C. thanks Vince Bojan for helpful discussions and comments in the analysis of XPS data.

Supporting Information Available: Figure A a wide scan XPS spectra for (a) = the system AMS/PMeT(500 Å)/$(HDT/CdSe)_1$/HDT, ***Device B***, and (b) = AMS/Ppy(20 Å)/$(HDT/CdSe)_3$/HDT, ***Device A***, after storage in air for 20 months and Figure B a close-up XPS survey spectra of Cd 3d core for ***Device B*** (a) and ***Device A*** (b). Note the absence of signal for cadmium oxide (2 pages, print/PDF). See any current masthead page for ordering and Web access instructions.

JA9806027

(51) Koehler, M.; Hümmelgen, I. A. *Appl. Phys. Lett*. **1997**, *70*, 3254.
(52) Heeger, J. A.; Parker, I. A.; Yang, Y. *Synthetic Metals* **1994**, *67*, 23.
(53) (a) Frank, A. J.; Glenis, S.; Nelson, A. J. *J. Phys. Chem*. **1989**, *93*, 3818. (b) Glenis, S.; Frank, A. J. *Synthetic Metals* **1989**, *28*, C681. (c) Frank, A. J.; Glenis, S. In *Photochemistry and Photoelectrochemistry of Organic and Inorganic Molecular Thin Films*; SPIE, 1991; pp 50−57. (d) Nguyen Cong, H.; Sene, C.; Chartier, P. *Solar Energy Materials and Solar Cells* **1993**, *29*, 209. (e) Nguyen Cong, H.; Sene, C.; Chartier, P. *Solar Energy Materials Solar Cells* **1993**, *30*, 127−138.
(54) (a) Frank, A. J.; Honda, K. *J. Phys. Chem*. **1982**, *86*, 1933. (b) Hagemeister, M. P.; White, H. S. *J. Phys. Chem*. **1987**, *91*, 150. (c) Tsamouras, D.; Dalas, E.; Sakkopoulos, S.; Vitoratos, E. *Appl. Surf. Sci*. **1993**, *65/66*, 388.
(55) Kumar, N. D.; Joshi, M. P.; Friend, C. S.; Prasad, P. N.; Burzynski, R. *Appl. Phys. Lett*. **1997**, *71*, 1388.
(56) Bowen Katari, J. E.; Colvin, V. L.; Alivisatos, A. P. In *Biomimetic Materials Chemistry*; Mann, S., Ed.; VCH: 1996.